Available online at www.sciencedirect.com

ScienceDirect

journal homepage: www.elsevier.com/locate/he

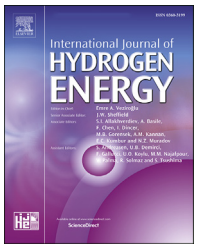

On the long-term stability of Pd-membranes with TiO_2 intermediate layers for H_2 purification

D. Sanz-Villanueva [a], D. Alique [a], A.J. Vizcaíno [a,*], J.A. Calles [a], R. Sanz [b]

[a] Department of Chemical, Energy and Mechanical Technology, Rey Juan Carlos University, Móstoles, Spain
[b] Department of Chemical and Environmental Technology, Rey Juan Carlos University, Móstoles, Spain

HIGHLIGHTS

- Pd-doped titania highly reduces the Pd-thickness for reaching fully dense membranes.
- TiO_2 barriers yield H_2 permeance up to $4.17 \cdot 10^{-4}$ mol/s m^2 $Pa^{0.5}$ and complete $\alpha_{H2/N2}$.
- Pd-doped titania allows stability for long-time operation up to 1000 h at 400 °C.
- Temperature above 450 °C leads to certain PdTi alloy and H_2 permeance decrease.

ARTICLE INFO

Article history:
Received 26 October 2021
Received in revised form
26 November 2021
Accepted 1 December 2021
Available online 23 December 2021

Keywords:
Composite-membrane
Palladium
Electroless plating
TiO_2
Intermediate layer
Membrane stability

ABSTRACT

This work addresses the use of TiO_2-based particles as an intermediate layer for reaching fully dense Pd-membranes by Electroless Pore-Plating for long-time hydrogen separation. Two different intermediate layers formed by raw and Pd-doped TiO_2 particles were considered. The estimated Pd-thickness of the composite membrane was reduced in half when the ceramic particles were doped with Pd nuclei before their incorporation onto the porous support by vacuum-assisted dip-coating. The real thickness of the top Pd-film was even lower (around 3 μm), as evidenced by the cross-section SEM images. However, a certain amount of palladium penetrates in some points of the porous structure of the support up to 50 μm in depth. In this manner, despite saving a noticeable amount of palladium during the membrane fabrication, lower H_2-permeance was found while permeating pure hydrogen from the inner to the outer surface of the membrane at 400 °C ($3.55 \cdot 10^{-4}$ against $4.59 \cdot 10^{-4}$ mol m^{-2} s^{-1} $Pa^{-0.5}$). Certain concentration-polarization was found in the case of feeding binary H_2–N_2 mixtures for all the conditions, especially in the case of reaching the porous support before the Pd-film during the permeation process. Similarly, the effect of using sweep gas is more significant when applied on the side where the Pd-film is placed. Besides, both membranes showed good mechanical stability for around 200 h, obtaining a complete H_2/N_2 ideal separation factor for the entire set of experiments. At this point, this value decreased up to around 400 for the membrane prepared with raw TiO_2 particles as intermediate layer (TiO_2/Pd). At the same time, complete selectivity was maintained up to 1000 h in case of using doped TiO_2 particles (Pd–TiO_2/Pd). However, a specific decrease in the H_2-permeate flux was found while operating at 450 °C due to a possible alloy between palladium and titanium that is not formed at a lower temperature (400 °C). Therefore, Pd–TiO_2/Pd membranes prepared by Electroless Pore-

* Corresponding author.
E-mail address: arturo.vizcaino@urjc.es (A.J. Vizcaíno).
https://doi.org/10.1016/j.ijhydene.2021.12.005

Plating could be very attractive to be used under stable operation in either independent separators or membrane reactors in which moderate temperatures are required.

Introduction

The potential of hydrogen as a versatile and clean energy vector is becoming a relevant topic in the last years [1,2] to replace progressively the use of fossil fuels with renewable energies [3,4]. Different studies show the potential of a wide variety of technologies to produce green hydrogen, such as water electrolysis [5], thermochemical water splitting [6], dark fermentation [7], biomass gasification [8], or biomass-derivatives reforming [9,10], among others. However, the contribution of all these technologies to hydrogen production is certainly residual due to their elevated and technological early stages [11]. In contrast, around 96% of profitable hydrogen is produced from fossil fuels via mature technologies such as steam reforming, partial oxidation, or gasification [3]. In many of these cases the generated hydrogen is typically accompanied by other byproducts, thus requiring an additional separation step to adjust its purity for each particular application [12]. These purification steps can be carried out by diverse technologies [13,14], although the use of hydrogen-selective membranes provides essential advantages in terms of energy consumption and versatility for a wide variety of production rates [15]. Additionally, these membranes can be implemented inside the reactors, thus combining both generation and separation processes in a single device denoted as membrane reactor [16–21].

In this context, many membrane materials are currently under research to be applied in both independent hydrogen separation units or membrane reactors [22]. However, those made of palladium or its alloys currently seem to prevail over other alternatives because of their thermal resistance, complete theoretical selectivity towards hydrogen, and moderate permeate fluxes [23,24]. Hydrogen permeation through these membranes can be typically expressed by the Sieverts' law (Eq. (1)) in the function of the permeation driving force and specific characteristics parameters of the membrane:

$$J_{H2} = \frac{Q'_{H2}}{t_{Pd}}\left(P_{H2,r}^{0.5} - P_{H2,p}^{0.5}\right) = Q_{H2}\left(P_{H2,r}^{0.5} - P_{H2,p}^{0.5}\right) \quad (1)$$

where J_{H2} is the permeate hydrogen flux, Q'_{H2} the membrane permeability, t the palladium thickness, Q_{H2} the H_2-permeance and $(P_{H2,r}^{0.5} - P_{H2,p}^{0.5})$ the driving force of the permeation process is expressed as the difference between the hydrogen partial pressures in both retentate and permeate sides (subscripts r and p, respectively) raised to the power of 0.5.

A wide variety of studies have demonstrated the potential of diverse Pd-based membranes to withstand reforming operating conditions with temperatures in the range of 350 and 600 °C and feed pressures up to 12 bar [25–29]. However, a prevalent solution has not been found up to now. Further improvements are still under research trying to decrease as much as possible the Pd-thickness to simultaneously reduce the overall cost of the membrane and increase its permeability while maintaining enough mechanical and thermal resistances [25]. The fabrication of composite membranes in which a relatively thin palladium film is incorporated onto porous support providing the required mechanical resistance is one of the preferred strategies to achieve the aforementioned goals [26,27]. The thinnest Pd-films are usually obtained using ceramic supports with a very smooth surface and narrow pore size distribution around a few nanometers [30]. However, their mechanical stability compromises their use when fitting in standard industrial steel devices [28,29]. These drawbacks can be overcome by using metallic supports like porous stainless steel (PSS) that ensure compatible thermal expansion coefficients between all the staked layers and enough mechanical robustness to be integrated into industrial facilities. However, the use of these metallic supports conditions the final Pd-thickness because of their larger pores up to several micrometers, wider pore size distribution, and higher roughness than those provided by the ceramic ones [31,32]. In addition, direct contact between Pd-films and metallic supports could provoke a degradation of the H_2-selective layer due to the interdiffusion and alloy of certain SS species into the palladium, mainly when the membrane operates for long times, hence drastically reducing the H_2-permeation through the membrane [33]. The incorporation of a wide variety of intermediate layers between the porous support and the top Pd-film has been proposed as an effective solution to overcome these problems, being possible to find barriers made of Al_2O_3 [30], SiO_2 [34,35], YSZ [33,36], zeolites [37,38], CeO_2 [37,39] or TiO_2 particles [33,40], among others. The last ones, formed by titania particles, attract great interest due to their relatively low cost and possible catalytic activity in specific processes such as photocatalytic hydrogen production from aqueous methanol solution [41,42].

Furthermore, the thermal expansion coefficient of TiO_2 is between 8.3 and 10.9 μstrain/°C, which is relatively close to the values provided by palladium (10.0 μstrain/°C) and 316 L SS (14.5–18.0 μstrain/°C), thus predicting a theoretical absence of stress between the different layers of the composite membrane under successive operation and thermal shutoff cycles [27]. However, the use of Pd-membranes containing TiO_2 intermediate layers requires a further discussion in depth. Despite the above-mentioned apparent benefits, some authors suggest a possible degradation of these membranes during permeation and reaction tests at specific operating conditions. In this context, Wei et al. [40] reported a stable H_2 permeation flux for at least 100 h in composite Pd-membranes in which PSS supports were coated with TiO_2 as an

intermediate barrier. Huang and Dittmeyer [33] found a possible alloy between palladium and titanium coming from the TiO_2 intermediate layer in similar membranes that provoked a decrease in the permeation capacity of these membranes. This effect could not be demonstrated conclusively due to the difficulties to characterize the possible PdTi alloy but justified the evolution of the permeation behavior. The use of other different ceramic intermediate layers during the membrane preparation led to more stable membranes. More recently, Fernandez et al. [43] stated a noticeable decrease in the H_2-permeability of composite PdAg membranes onto alumina tubular supports. At the same time, they operated inside a fluidized-bed membrane reactor due to the multiple hits of catalyst particles, basically made of TiO_2, against the PdAg film and chemical interaction between them. In this context, Arratibel et al. [44] incorporated a top mesoporous YSZ/γ-Al_2O_3 layer onto this type of membrane, thus protecting the PdAg surface against hitting with the fluidized catalyst particles and avoiding membrane degradation. Nevertheless, all these insights seem to depend on characteristic membrane properties and particular experimental conditions, so the use of TiO_2 intermediate layers should not be dismissed entirely before further research.

In this context, the current study goes into detail about the permeation behavior of Pd-based composite membranes. First, the external morphology of raw PSS supports is modified by incorporating TiO_2 intermediate layers to elucidate the conditions in which titanium and palladium could interact, negatively affecting the overall membrane performance. Two different titania particles, raw commercial or doped with finely distributed Pd-nuclei onto their surface, are considered to be used as an intermediate layer before incorporating the palladium through Electroless Pore-Plating from opposite sides of the modified supports for the first time. As a result, the permeation behavior of these membranes has been thoroughly analyzed in multiple conditions, including diverse pressure driving forces, temperatures, the contrary direction of the permeate flux, gas mixtures, and sweep-gas flow rates. Moreover, a detailed analysis of the long-term stability of the membranes combined with their morphological characterization is also presented.

Experimental procedure

Membrane fabrication

As previously indicated, two different types of composite Pd-membranes were prepared onto PSS supports, including intermediate layers basically formed by TiO_2 particles. Commercial PSS supports with tubular geometry (12.9 mm OD, 1.9 mm wall thickness, and 600 mm in length) were purchased from Mott Metallurgical corp. (Farmington, Connecticut, United States of America). The raw support, classified as 0.1 μm media-grade, presents a homogeneous porous structure with porosity around 20% and an average pore mouth diameter on the external surface <4 μm, although it is also frequent to find some noticeably bigger pore mouths.

First, the raw supports were cut into smaller samples (30 mm in length per unit) and their opposite ends were perfectly polished to ensure a good future fitting into both deposition and permeation cells before starting the membrane preparation. Once it is completed, each sample is subjected to several consecutive treatments to clean possible dirty coming from previous steps, modify the original morphology and incorporate the H_2-selective palladium dense film, as schematically depicted in Fig. 1. Further details about each particular step carried out during the fabrication of membranes are collected in the next sub-sections, as well as equipment and techniques considered for their characterization.

Initial conditioning of supports

The initial conditioning of PSS supports starts with their cleaning by successive immersions in 0.1 M sodium hydroxide and 0.1 M hydrochloric acid for 5 min followed by an additional one in ethanol (96% v/v) for 15 min. These immersions are carried out at 60 °C under sonication, while intermediate rinsing in distilled water between each step is applied to avoid contamination between solutions. Then, the cleaned pieces are dried overnight at 110 °C and then calcined in air at 600 °C for 12 h to generate a first preventive interdiffusion layer of Fe–Cr oxides (PSS-OXI). Further details about these conditioning procedures can be found in our previous studies [31,45].

Incorporation of TiO_2 intermediate layers

As previously discussed in the introduction, the incorporation of additional intermediate layers formed by ceramic particles could prepare thinner Pd-composite membranes besides avoiding possible intermetallic diffusion between PSS and Pd layers during operation. In this work, commercial TiO_2 powders with a particle size of around 10 μm from GetNano Materials (Saint-Cannat, France) have been considered to be used as ceramic intermediate layers. The powders were incorporated onto the external surface of oxidized PSS supports by two consecutive recurrences of vacuum-assisted dip-coating (VA-DC) for 5 min from a suspension containing a particle load of 15% w/w with 2% w/w of poly(vinyl alcohol) (PVA). To avoid the incorporation of particles onto the lumen side of the supports, this zone was sealed with silicone gaskets and connected to the vacuum line before initiating the coating process. The entire VA-DC procedure was carried out at room conditions with an intermediate drying step at room temperature for 2 h. The vacuum was applied only during the last minute of the second dip-coating recurrence when some particles were already incorporated onto the external surface of OXI-PSS support. Then, the modified supports were dried overnight at 110 °C and calcined in air at 500 °C for 5 h to ensure complete removal of PVA.

At this point, it should be noted that two different intermediate layers based on TiO_2 particles were considered in this study. The first one consists of the direct incorporation of the raw commercial TiO_2 particles accordingly to the above-mentioned general VA-DC procedure (TiO_2). On the other hand, an additional intermediate layer in which the ceramic particles were previously doped with Pd nuclei before their incorporation onto the porous support was also generated (Pd–TiO_2). In this case, 6.7 g of TiO_2 particles were immersed in 90 mL of an aqueous acidic solution containing a certain amount of palladium (0.1 g/L $PdCl_2$, 1 mL/L HCl 35% v/v). Then

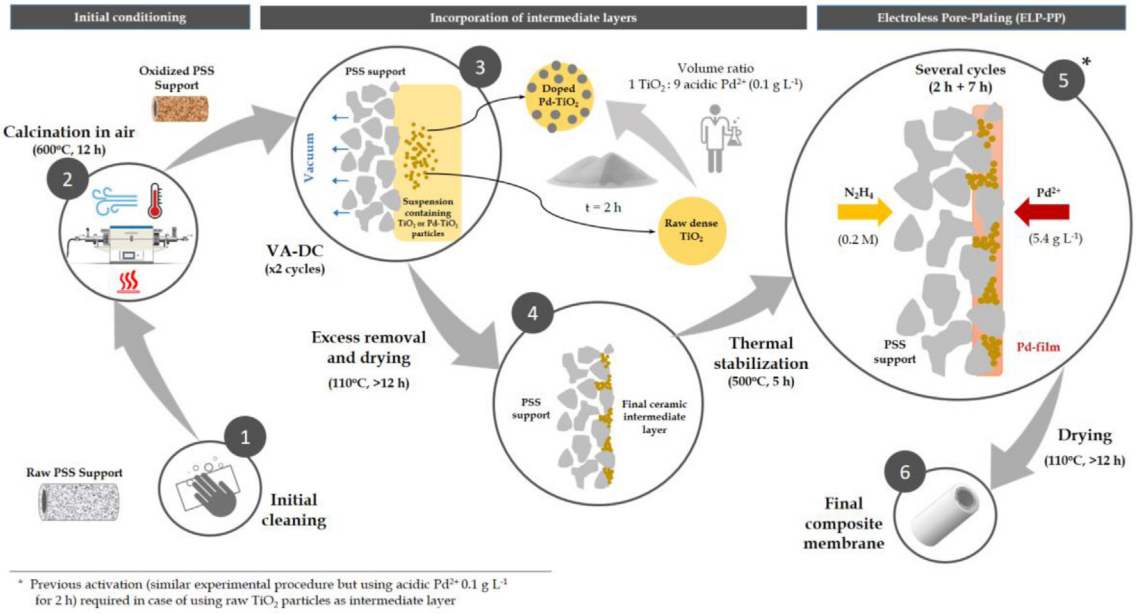

Fig. 1 – Schematic experimental procedure carried out for the membrane fabrication.

3 mL of a solution of hydrazine 0.2 M in ammonia 2 M is added to provoke the reduction of palladium ions while maintaining under stirring at room temperature for 2 h. Finally, the suspension was filtered and dried overnight at 110 °C before being used according to the previously described VA-DC general procedure.

Pd-film deposition

The palladium layer was deposited by Electroless Pore-Plating (ELP-PP) accordingly to the procedure reported by our research group in several previous studies [46–48]. It is important to note that any electroless plating procedure requires a previous activation of the porous substrate with fine Pd-nuclei well distributed along the entire surface to ensure a subsequent homogeneous deposition of the final dense Pd-film [49]. This activation process was carried out by direct reduction of an aqueous acidic solution containing the Pd source (0.1 g/L $PdCl_2$ and 1 mL/L HCl 35% v/v) with a 0.2 M hydrazine solution in ammonia 2 M, being possible to distinguish two different cases in the function of the considered intermediate layer, TiO_2 or Pd–TiO_2. In the first case, the activation of the support containing raw TiO_2 particles as intermediate layer consists of feeding each described solution (Pd source and reducing) from opposite sides of the modified support. Particularly, the Pd source is placed around the external side of the porous support while the reducing solution is added from the lumen side. In this manner, the formation of the first Pd nuclei is forced to be produced around pore areas. This activation process is carried out at room temperature for 2 h. After that, the activated support is rinsed with distilled water and finally dried overnight at 110 °C. However, this procedure can be omitted when considering the use of activated ceramic particles before VA-DC (Pd–TiO_2), precisely because the required fine first Pd nuclei are previously incorporated.

Independently of the selected alternative to generate these first Pd nuclei, the final dense Pd film is incorporated by ELP-PP. This technique, carried out at 60 °C, is characterized by feeding both plating solutions, Pd source (5.4 g/L $PdCl_2$, 390 mL/L NH_4OH 32% and 70 g/L EDTA) and reducing agent (N_2H_4 0.2 M), from opposite sides of the porous support to force the chemical reaction just inside the pores or around their neighbor areas. The process was repeated a certain number of recurrences until all pores became completely sealed by palladium particles, thus obtaining a fully dense membrane and the chemical reaction automatically stops due to the impossibility of meeting the solutions. The membranes prepared with raw TiO_2 and Pd–TiO_2 particles as intermediate layers were denoted as TiO_2/Pd and Pd–TiO_2/Pd, respectively.

Physical membrane characterization

The main physical properties of materials and membranes so prepared were completely characterized before and after being used in permeation. First, the particle size distribution of commercial TiO_2 considered for the preparation of intermediate layers was determined with a NanoPlus-3 particle size analyzer. The palladium amount incorporated onto the porous supports during ELP-PP was determined by gravimetric analyses (electronic balance Kern & Sohn ABS-4 with a precision of ±0.0001 g) to estimate the average thickness of the H_2-selective layer by considering homogeneous plating around the external surface of the supports. Moreover, the external morphology of the membranes at different stages of their fabrication process was analyzed by Scanning Electron Microscopy with a Philips XL30 ESEM microscope. The cross-section view of the membranes was also obtained by Hitachi 3000-n microscope equipped with Bruker Quantax EDS analyzer XFlash 6130 to determine the real thickness and homogeneity of each incorporated layer after being used in permeation. Moreover, further information was also extracted from these images, analyzing the variation of membrane composition in the radial direction.

Permeation measurements

The permeation behavior of modified porous supports and final dense composite-membranes was determined in a homemade setup designed for testing pure gases or binary H_2–N_2 mixtures at multiple operating conditions, as described elsewhere [46]. Both supports and membranes are placed in a 316 L SS permeation cell, sealing their extremes with graphite O-rings to separate permeate and retentate sides. The operating temperature is adjusted within the range of 350–450 °C thanks to a thermocouple placed close to the external surface of the membrane and an external electrical furnace. The system can be fed with pure nitrogen, hydrogen, or binary mixtures with variable composition using mass-flow meters Bronkhorst High-Tech B.V. with a maximum capacity of 400 NmL/min. Moreover, this feed gas stream can be introduced from the inner or the outer side of the membrane thanks to the presence of two four-way valves in the connections, thus being possible to analyze contrary permeation modes, denoted as "in-out" or "out-in", respectively. In all experiments, the permeate side, collected from the opposite side to the inlet stream reach the membrane, was maintained at atmospheric pressure, being possible to introduce an additional sweep gas. The retentate pressure was regulated thanks to an EL-PRESS Bronkhorst High-Tech B.V. backpressure controller to reach pressure-driving forces up to 2.5 bar during permeation experiments. The permeate fluxes was measured by a Horiba SF-2U flow meter with a precision of ±0.01 Nml·min^{-1}.

Results and discussion

The most relevant results obtained in the present study have been structured in three different sections focused on: i) membrane morphology, ii) general permeation behavior, and iii) long-term performance of composite-membranes fabricated by using raw or doped TiO_2 particles as intermediate layer.

Membrane morphology

As previously described in the experimental section, two different TiO_2 particles were incorporated by VA-DC as intermediate layer between PSS supports and final ELP-PP Pd-films. The average size of these particles was determined at around 3–4 μm, not obtaining significant differences before and after their activation with Pd-nuclei. Further details about this preliminary characterization of TiO_2 and Pd–TiO_2 particles can be found as supporting information (Fig. S1). Independently of the considered particles, a similar process to incorporate the intermediate layer onto the porous support was carried out by using suspensions with 15% w/w particle load during VA-DC. At these conditions, considering the similar morphology of the ceramic particles and incorporation process, similar incorporation onto the porous supports was also reached with total weight per membrane length around 5.07 and 4.73 mg/cm for TiO_2 and Pd/TiO_2 samples, respectively. As can be seen, a minimum difference of around 7% was obtained, being possible to attribute this slight deviation to the intrinsic variability of the incorporation process at laboratory scale instead of a real influence of replacing the raw commercial TiO_2 by Pd–TiO_2 particles.

The particular morphology of the external surface reached on the porous supports after incorporating these intermediate layers is shown in Fig. 2. In both cases, the ceramic particles were incorporated homogeneously into most of the original pores of the support, thus reducing both average pore-mouth diameter and external roughness. As previously suspected by gravimetric analysis, no significant differences are observed in the samples, denoting that the presence of Pd nuclei onto the raw commercial TiO_2 particles does not affect their incorporation as intermediate layer.

The permeation capacity of these modified supports has also been analyzed through some control tests feeding pure N_2 at room temperature and setting the pressure-driving force as 1.0 bar. For a better comparison, the results reached when testing raw PSS supports, oxidized ones in air atmosphere at 600 °C for 12 h and other modified supports with intermediate layers made of CeO_2 [50] and SBA-15 [48] have also been included together with the new membranes presented for the first time in this work (Fig. 3). As can be seen, the original permeation capacity of raw PSS supports progressively decreases as Fe–Cr oxide or ceramic intermediate layers were incorporated. In the first case, when testing PSS-OXI supports, a very slight decrease in the original permeation capacity was obtained due to the ultra-low thickness of the top Fe–Cr oxide layer generated onto each SS grain and limited surface morphology modification [51]. This effect was noticeably more pronounced for the membranes in which ceramic intermediate layers were incorporated by VA-DC because of the greater modification of the original textural properties of supports (decrease of porosity and average pore-mouth diameter). Particularly focusing on the modified supports with titania-based intermediate layers, a very similar permeation capacity was obtained, thus confirming the previous insights in which it was concluded that doping TiO_2 with Pd does not affect in a relevant manner to its incorporation onto the support as intermediate layer. Compared with other ceramic barriers included in the figure, a certain increase in the permeation capacity of around 3% was reached over the sample with the SBA-15 intermediate layer, but a reduction of 20% was produced concerning the CeO_2 sample. This trend can be justified by the average particle size of the ceramic particles. An average diameter of TiO_2-based particles around 3–4 μm was observed (with a bimodal distribution around diameters of 320–350 nm and 15.5–16.8 μm), while this parameter for CeO_2-based particles was maintained around 10 μm. Thus, this variation could justify greater compaction of TiO_2 particles during VA-DC and, consequently, a slight decrease in the permeation capacity of modified supports.

Once the modified porous supports with different TiO_2-based intermediate layers were characterized to ensure their convenience for the composite-membrane preparation, the final morphology of the membranes after the palladium plating by ELP-PP has also been discussed. Two different composite-membranes, denoted as TiO_2/Pd and Pd–TiO_2/Pd due to the use of respective raw TiO_2 and Pd-doped TiO_2 materials as intermediate layers, can be distinguished. At this point, it is important to remember that each membrane only is considered completed when its weight maintains unaltered after a

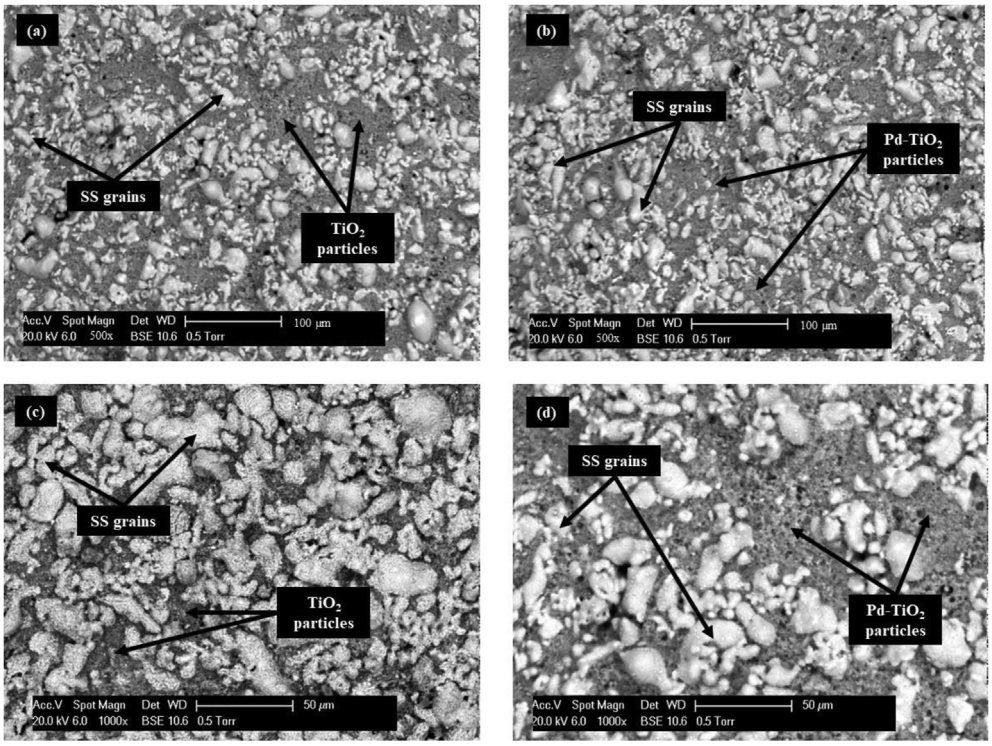

Fig. 2 – External morphology of modified OXI-PSS supports with TiO_2 (a, c) and Pd–TiO_2 (b, d) particles as intermediate layer.

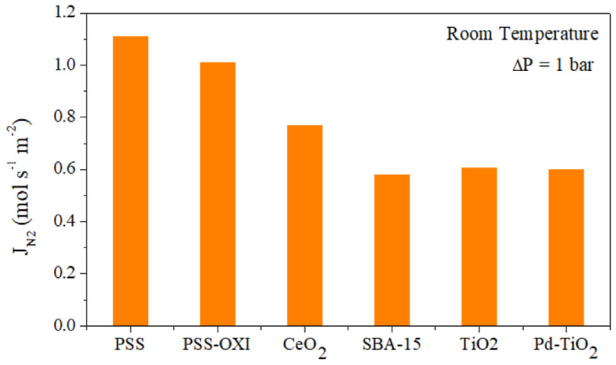

Fig. 3 – Permeation capacity (room temperature, $\Delta P = 1$ bar) of original PSS support and modified ones by oxidation (PSS-OXI) or incorporation of diverse ceramic intermediate layers: CeO_2, SBA-15, TiO_2, and Pd–TiO_2).

recurrence of the ELP-PP process (t = 7 h), thus suggesting the complete blockage of all the pores with palladium. This fact is corroborated by rapid leakage tests with helium in ethanol at room temperature and retentate pressures up to 3.0 barg. Complete retention of helium at these conditions was reached for both membranes. Fig. 4 collects the SEM micrographs taken onto the reached external surface after the pallium deposition. The formation of an external top Pd-film with good continuity and homogeneity can be observed in both membranes, independently of incorporating TiO_2 or Pd–TiO_2 intermediate layers. This morphology is typical of other ELP-PP membranes, being possible to explain the formation of this top coating by the presence of a wide variety of diameters in the porous support, despite incorporating the intermediate layers [49].

Regardless of the similarities found on the external morphology exhibited by TiO_2/Pd and Pd–TiO_2/Pd membranes, noticeably differences in the Pd-thickness estimated by gravimetric analyses ($t_{Pd,e}$) deserve to be further discussed. Thus, a significantly lower Pd-thickness of 9.7 μm was required to prepare a fully dense ELP-PP membrane by using Pd–TiO_2 particles instead of the raw commercial ones, when this thickness increased up to 19.4 μm. These results agree with previous works in which a considerable reduction of the final Pd-thickness of ELP-PP membranes was achieved by doping CeO_2 [52] or SBA-15 particles [48] with Pd-nuclei before being incorporated as intermediate layer onto the porous supports. In general, the presence of these Pd nuclei onto the particles enhances the subsequent Pd plating around them, previously incorporated into the pores of the support, thus reaching a more effective activation compared with a traditional process.

Permeation tests

The permeation behavior of both membranes including TiO_2-based intermediate layers has been studied for temperatures and pressure-driving forces in the range of 350–450 °C and 0.5–2.5 bar, respectively. These experiments were carried out by feeding pure gases, N_2 and H_2, and binary mixtures with diverse compositions considering two different permeation modes: i) in-out (permeation flux from the lumen to the shell side) and ii) out-in (permeation flux from the shell to the lumen side). In general, no sweep gas was used to collect the

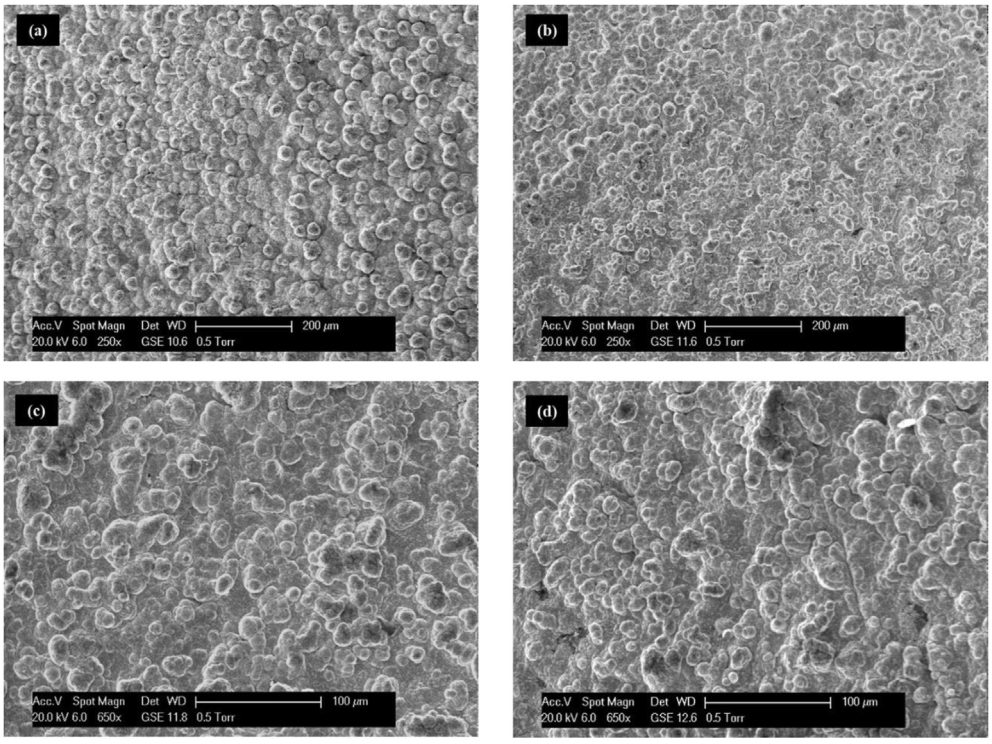

Fig. 4 – External morphology of TiO_2/Pd (a, c) and Pd–TiO_2/Pd (b, d) membranes after Pd-plating by ELP-PP.

permeate, although its possible influence on the results was also evaluated.

General permeation behavior

First, it should be emphasized that no permeate flux was detected when feeding N_2 at the reference temperature of 400 °C and pressure-driving forces up to 3.0 bar for both contrary operation modes, in-out and out-in, thus maintaining the preliminary good quality of the ELP-PP Pd-films incorporated on both membranes (TiO_2/Pd and Pd–TiO_2/Pd) also at higher temperatures.

Under this initial premise, Fig. 5 exhibits the permeate fluxes reached at 400 °C for each membrane when pure H_2 is fed and both contrary operating modes out-in and in-out are considered. In all these cases, no sweep gas was applied to the permeate side. In general, a good linear fitting of experimental data with pressure is obtained for both membranes and operating modes, although without intercepting in (0,0) as suggested by Sieverts' law. This characteristic behavior of diverse ELP-PP has been widely addressed in previous works published [34,53]. Briefly, this effect can be connected with the penetration of Pd-film into the pores of the support due to the nature of plating process, making it difficult for a precise determination of pressures just on the surface of the metal in both permeate and retentate sides as required by the theoretical equation. In this context, considering an additional internal resistance against the H_2 permeation through the membrane could account for this effect. In fact, higher resistances appear as increasing the Pd infiltration inside the pores, as concluded in previous studies while varying the hydrazine concentration during ELP-PP [51]. In this case, a certain increase of this internal resistance from 8 to 15 $Pa^{0.5}$ to around 18 $Pa^{0.5}$ can be observed when the intermediate layer is formed by Pd–TiO_2 instead of raw TiO_2 particles. This fact suggests a greater infiltration of Pd-film into the pores during ELP-PP thanks to the presence of fine well-distributed Pd nuclei around the particles before being incorporated onto the porous support. This hypothesis was also confirmed by analyzing different cross-sectional images, included and discussed in the next section. In this context, H_2-permeances of $4.59 \cdot 10^{-4}$ and $3.55 \cdot 10^{-4}$ mol s^{-1} m^{-1} $Pa^{-0.5}$ have been calculated for TiO_2/Pd and Pd–TiO_2/Pd, respectively, when permeating from the inner to the outer surface of the membranes (in-out mode). This fact really attracts attention because higher permeance

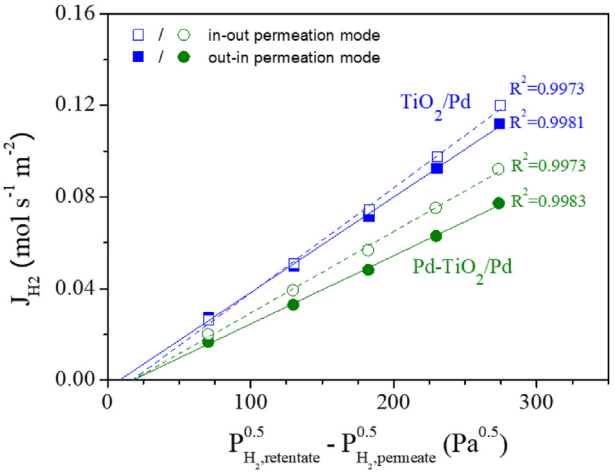

Fig. 5 – Hydrogen permeation of TiO_2/Pd and Pd–TiO_2/Pd membranes at 400 °C.

was obtained for the apparently thicker membrane, maintaining this trend when reversing the permeation flux direction from in-out to out-in mode ($4.16 \cdot 10^{-4}$ against $2.97 \cdot 10^{-4}$ mol s^{-1} m^{-1} $Pa^{-0.5}$). Once again, this fact can be explained by the palladium infiltration into the pores of the support. Thus, the use of Pd–TiO_2 particles saves palladium during ELP-PP to reach a fully dense membrane (Pd–TiO_2/Pd, $t_{Pd,e}$ = 9.7 μm) in comparison with considering raw ceramic particles (TiO_2/Pd, $t_{Pd,e}$ = 19.4 μm), but provokes a greater infiltration of the metal into the pores. Therefore, hydrogen has to diffuse through a thicker effective distance in the Pd bulk after being dissociated onto its surface. Alique et al. [54] described a similar behavior for ELP-PP membranes prepared onto asymmetric alumina supports, in which they exhibited permeate H_2 fluxes equivalent to other thicker membranes due to a greater infiltration into the pores of the substrate.

Focusing on the influence of the permeation direction, higher fluxes were reached for both membranes, in general, while permeating from the inner to the outer side. However, in-out and out-in configurations have a different contribution for each particular membrane. Thus, the effect of the permeation direction is very slight for TiO_2/Pd, which exhibits the highest permeation capacity. On the contrary, this effect is more pronounced for Pd–TiO_2/Pd with a lower permeation capacity eventually caused by a greater infiltration of palladium inside the pores. In all cases, this effect can be justified by the uncertainty in determining the real pressure just on both surfaces of the Pd-film, as addressed in previous works [46,48]. The contribution of this effect is less relevant as the Pd-infiltration inside the pores of the support decreased of the thickness of the top Pd-film increases. Besides, all these experiments demonstrate the good mechanical stability of TiO_2/Pd and Pd–TiO_2/Pd membranes despite operating at experimental conditions in which tensile stress is generated on the palladium. Despite this fact, no delamination was observed and a complete nitrogen tightness was maintained. Therefore, a complete ideal separation factor ($\alpha_{H2/N2}$) can be assumed up to pressure-driving forces of around 2.5 bar for both membranes.

Fig. 6 collects a series of experiments at temperatures ranged from 350 to 450 °C with a general similar behavior to previously addressed for both membranes. For higher clarity, only the data reached for one permeation direction (in-out mode) are depicted. The linearly of experimental data was maintained for all the conditions and an Arrhenius type-dependence with the temperature was obtained, with increasing permeate fluxes for higher temperatures and very similar activation energies 14.7–14.9 kJ mol^{-1}, within the typical range shown by other Pd-based membranes [27]. It should be noted that the mechanical stability of the membranes and initial H_2-selectivity was maintained after this set of experiments.

To conclude this section, Table 1 collects the permeation behavior exhibited for different Pd-based membranes prepared by electroless plating onto PSS supports modified with a wide variety of materials as intermediate layer. It should be noted that a rigorous comparison is certainly difficult because of the different morphological properties of the membranes, multiple operating conditions at which they were tested, and finally reached H_2-selectivity. The Pd-thickness typically ranges between 5 and 20 μm, depending on the morphological

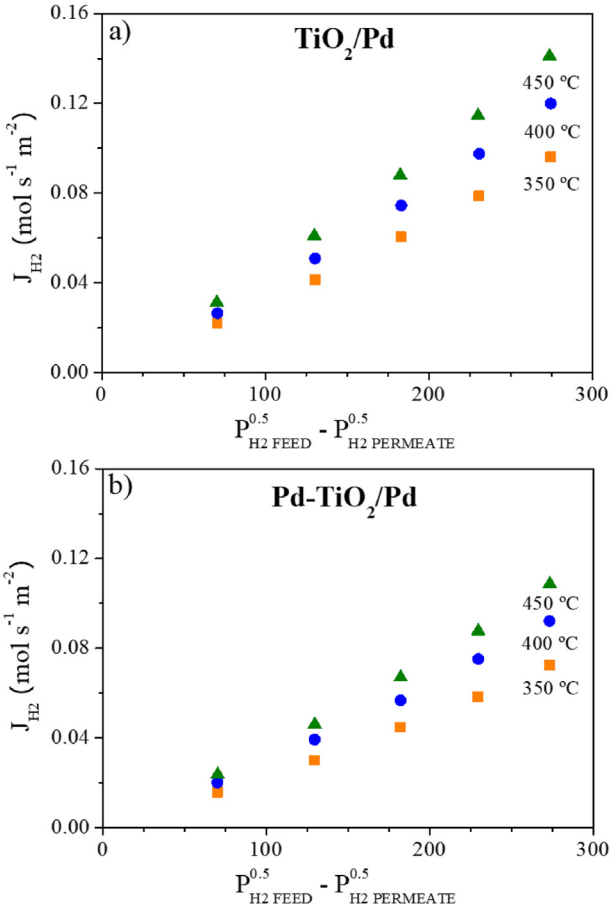

Fig. 6 – Temperature influence the permeation behavior of membranes: a) TiO_2/Pd and b) Pd–TiO_2/Pd.

properties reached on raw PSS supports after the incorporation of the intermediate layers. In general, thinner Pd layers leads to higher H_2-permeation capacity, although some exceptions to this general trend can also appreciate precisely due to the specific morphology of final Pd-films (as occurring with membranes prepared in this work, prepared by ELP-PP) or limited H_2-selectivity (typically expressed as H_2/N_2 ideal separation factor, $\alpha_{H2/N2}$). Anyway, it can be confirmed that membranes containing TiO_2-based intermediate layers prepared in this study exhibit a complete ideal selectivity to hydrogen (taking into account the minimum detection limit of the bubble-soap flow meter used during permeation of nitrogen, 1 NmL/h) and maintain a H_2-permeation capacity within the typical values provided by other membranes from literature.

Tests with H_2/N_2 mixtures

After addressing the general permeation behavior of the membranes when feeding pure gases, complementary permeation tests with H_2/N_2 mixtures were also carried out. The new experiments were performed by feeding mixtures containing 10–30% N_2 at 400 °C, pressure driving forces in the range 0.5–2.5, and considering both contrary permeation configurations, in-out, and in-out.

First, it should be noted that a complete H_2-selectivity was maintained for the entire set of experiments since no nitrogen

Table 1 – Permeation behavior of Pd-composite membranes prepared onto PSS supports modified with different intermediate layers.

Membrane	Preparation method	t_{Pd} (μm)	T (°C)	ΔP (kPa)	Permeation capacity (mol m^{-2} s^{-1} $Pa^{-0.5}$)	$\alpha_{H2/N2}$	Ref.
(–)/Pd	ELP	10	400	100–700	$8.96 \cdot 10^{-4}$ [(a)]	11,800	[55]
YSZ/Pd	ELP	13.8	350–450	30–250	$2.80–4.75 \cdot 10^{-4}$ [(a)]	∞	[36]
YSZ/Pd	ELP	20	400	0–100	$6.45 \cdot 10^{-4}$ [(a)]	340–400	[56]
Al_2O_3/Pd	ELP	4.4	500	800	$2.94 \cdot 10^{-3}$	1,124[(b)]	[32]
Silicalite-1/Pd	ELP	5.5	450	0–300	$1.42 \cdot 10^{-4}$	∞	[34]
Zeolite NaA/Pd	ELP	19	450	50	$1.1 \cdot 10^{-3}$	608	[57]
Pd-SBA-15/Pd	ELP-PP	7.1	400	50–250	$3.81 \cdot 10^{-4}$	≥2550	[48]
CeO_2/Pd	ELP	13	500	100–200	$3.38 \cdot 10^{-5}$ [(a)]	∞	[58]
Pd–CeO_2/Pd	ELP-PP	9.1	350–450	100–200	$4.46–6.39 \cdot 10^{-4}$	≥10,000	[52]
TiO_2/Pd	ELP-PP	19.4	350–450	50–250	$3.64–5.38 \cdot 10^{-4}$	∞	This work
Pd–TiO_2/Pd	ELP-PP	9.7	350–450	50–250	$2.80–4.17 \cdot 10^{-4}$	∞	This work

Permeation: [(a)] Calculated values from original ones given in a different format.
Ideal separation factor: [(b)] H_2/He.

was found in the permeate stream by gas chromatography. Then, H_2-permeance was determined from a linear fitting of reached H_2 fluxes against applied pressure driving forces for each experimental condition. All results are collected in Fig. 7, representing the ratio of particular H_2-permeances reached when feeding binary mixtures with diverse N_2 contents (k_i) and the reference one reached by feeding pure H_2 (k_{H2}).

Despite N_2 is an inert gas that does not interact with the membrane in a significant manner, it is well-known that its presence typically causes an H_2-permeance decrease due to a concentration-polarization effect [37]. This general effect is observed for the membranes included in this work, although with a different contribution depending on the particular membrane and permeation configuration. In fact, the negative effect of feeding N_2–H_2 mixtures, especially for increasing nitrogen contents, becomes more relevant when hydrogen permeate from the lumen to the shell side of the permeation cell (mode in-out), even considering that H_2-permeances reached with this configuration are maintained always higher than in case of working on the contrary configuration. This behavior could be explained by the effect of the porous structure provided by both PSS support and TiO_2 intermediate layers during the overall permeation process. In this manner, the H_2/N_2 mixture needs to pass through the porous structure before reaching the Pd film, where only hydrogen can permeate, according to the in-out configuration. Since nitrogen cannot diffuse through the bulk palladium, the rejected molecules need to go forward towards the retentate, making the permeation of additional hydrogen progressively more difficult and hence increasing the concentration-polarization. This situation turns into an overall decrease of H_2-permeance during permeation. This negative concentration-polarization effect has a lower contribution while permeating on the contrary direction, out-in configuration. In this case, the gas mixture reaches the Pd-film before passing through the porous media, so non-permeable nitrogen can be moved away from the Pd-surface in a relatively easier manner by the feed stream. All these experiments extended for around 120 h and the integrity of membrane Pd–TiO_2/Pd was maintained for the entire set of experiments, although membrane TiO_2/Pd evidenced a certain deterioration with a decrease in H_2-selectivity up to $\alpha_{H2/N2} \approx 400$ for ΔP = 2.5 bar. Therefore, it can be concluded that a previous activation of the TiO_2 particles used for the intermediate layers with Pd nuclei extends the lifespan of the composite membranes obtained by ELP-PP.

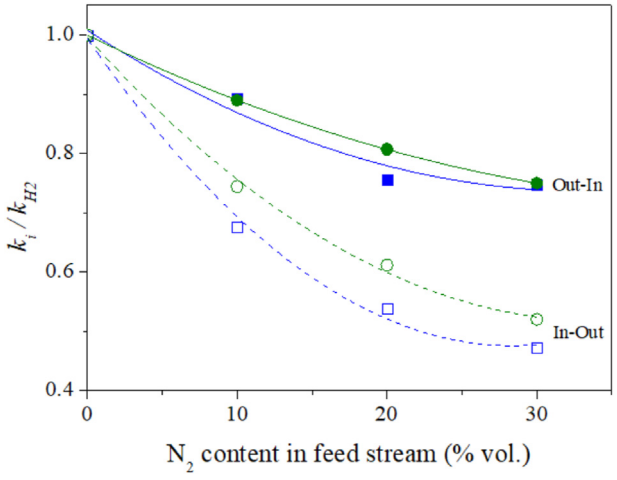

Fig. 7 – Influence of feeding binary H_2/N_2 mixtures for TiO_2/Pd (squares, ■/□) and Pd–TiO_2/Pd (circles, ●/○) membranes.

On the other hand, the effect of using a sweep gas was also studied for the membrane Pd–TiO_2/Pd. These additional experiments were performed at 400 °C for both in-out and out-in permeation modes by feeding 250 NmL/min pure hydrogen and various sweep gas flow rates within the range 0–150 mL/min. Fig. 8 collects all the results obtained from these experiments at pressure differences of 1–2 bar between retentate and permeate sides. These results are expressed as the ratio between the permeate when using sweep gas (Q_{H2}*) and the reference value at analogous conditions without sweep gas (Q_{H2}). In general, it can be stated that H_2-permeation increases as the sweep gas flow rate does, although a certain stabilization seems to be reached for sweep gas flow rates greater than 70 NmL/min. This trend can be explained by the variation in the real driving force reached for each experiment when sweep gas is used. For a constant pressure on the retentate side, an increase of the sweep gas flow rate provokes a

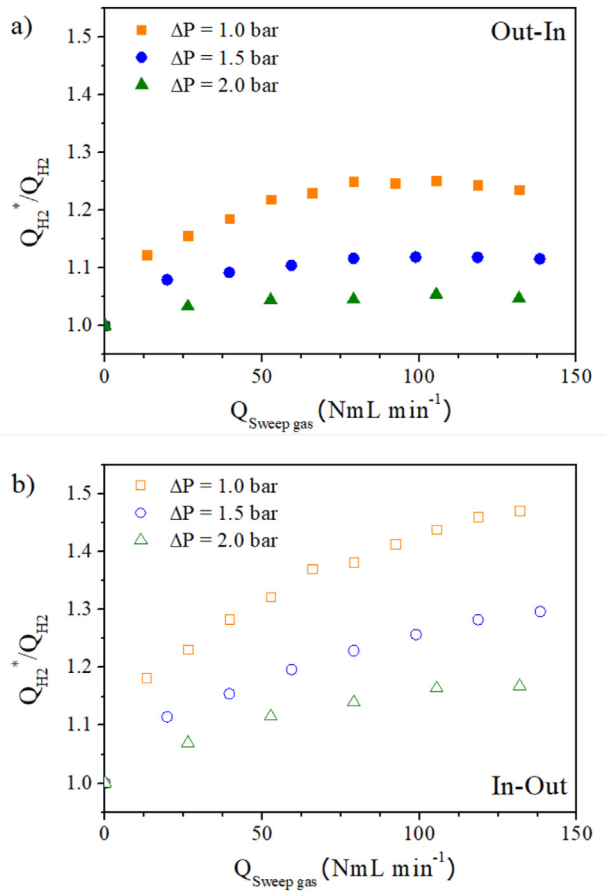

Fig. 8 – Permeation behavior of membrane Pd–TiO2/Pd using H_2 as feed and N_2 as sweep gas at 400 °C.

dilution of the permeate stream, a reduction in H_2 partial pressure at permeate side, and, hence, an increase of the overall pressure driving force. Once the sweep gas flow rate is high enough, a very diluted permeate is reached and the contribution on the hydrogen permeation of further dilution grades becomes limited. Focusing on the behavior obtained for different pressures, it can be observed that the possible benefits on H_2-permeance reached when using an inert sweep gas becomes lower as the pressure increases. It can be explained by the higher initial permeation reached as pressures increase and, consequently, the lower dilution rate generated on the permeate side by a certain sweep-gas flow rate. Finally, it is also important to address the different behavior obtained while operating in contrary in-out and out-in permeation configurations. A greater benefit of using sweep gas during permeation was reached when collecting the permeate flux from the external side of the membrane (in-out mode). In these cases, the sweep gas flow rapidly cleans the external surface of the top Pd-film, thus maintaining a reduced H_2 pressure just on the metal surface very close to the average value calculated for the bulk gas phase. In contrast, the presence of a porous media between the area where the sweep gas is flowing through and the Pd-surface makes the dilution more difficult just on the membrane film and, as a consequence, the reduction on the real pressure driving force becomes limited [59].

Long-term stability and post-permeation characterization

After the previous tests, the long-term stability of the Pd–TiO_2/Pd membrane was studied at ΔP = 1 bar, T = 400–450 °C, and out-in configuration for several hundred hours. Fig. 9 presents the variation of permeated H_2 with time for each temperature condition.

Before starting to discuss the results shown in Fig. 9, it should be highlighted that a complete H_2-selectivity was maintained during the entire set of experiments, so the membrane remained certainly stable, at least in terms of its mechanical integrity. The first 160 h were dedicated to previous tests with pure gases and mixtures, as prior detailed. After that, the H_2 permeate flux trends to be maintained stable around 0.051 mol s^{-1} m^{-2} at 400 °C for around 200 h. A certain increase can be also appreciated during the first period of around 50 h despite all the previous experiments probably due to a reconditioning of the membrane. However, this stability seems to be dependent on the experimental temperature, decreasing the permeate flux with an almost linear trend after around 50 h when the temperature increases from 400 to 450 °C. This negative effect stopped when the initial temperature of the experiment, 400 °C, was settled on again. At these conditions, an almost constant permeation flux was maintained for another 200 h, although the initial permeation capacity of the membrane was impossible to be recovered. This behavior suggests that higher temperatures provoke an irreversible degradation of the membrane that loses certain permeation capacity despite maintaining a complete H_2-selectivity. Dismissing a possible intermetallic diffusion between PSS components and palladium due to the presence of a first oxide layer (as evidenced in previous studies working at analogous conditions [45]) and a TiO_2 barrier, an interaction between the ceramic barrier and the selective film at 450 °C is suspected. In fact, several researchers suggest a possible alloy between titanium and palladium at certain operating conditions that turn into an overall decrease of H_2-permeance [33,43].

For better understanding of the impact of this phenomenon on the membrane performance, the behavior of the Pd–TiO_2/Pd membrane presented in this study is compared with the

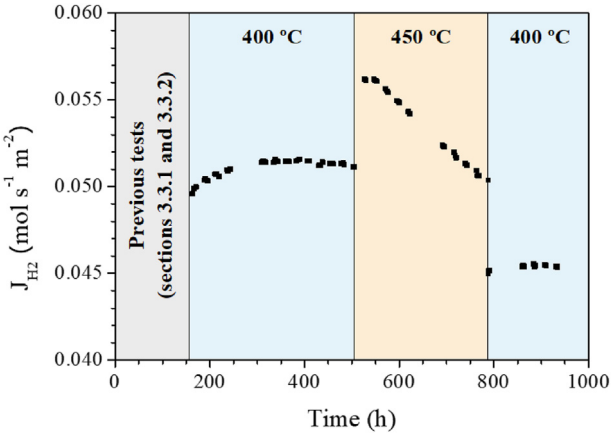

Fig. 9 – Long-term stability of membrane Pd–TiO_2/Pd (ΔP = 1 bar, out-in permeation mode).

performance of other membranes incorporating also TiO_2 intermediate layers. The H_2 permeance of Pd–TiO_2/Pd at 400 °C remains stable around $3.6 \cdot 10^{-4}$ mol s^{-1} $m^{-2} \cdot Pa^{-0.5}$ for 500 h with complete H_2-selectivity. A membrane with similar structure reported by Wei et al. [40] also exhibited a good stability at 400 °C, although it should be noted that a shorter testing time of 100 h was considered. This membrane presented higher permeance ($1.5 \cdot 10^{-3}$ mol s^{-1} $m^{-2} \cdot Pa^{-0.5}$) than the reported one by this research, although the H_2/N_2 ideal selectivity was limited in the range of 200–825. Huang and Dittmeyer [33] analyzed membranes containing different barrier layers. In that containing TiO_2, they detected a variation of the intermediate layer composition within a region in contact with the palladium layer after exposure to hydrogen at 600 °C for several days, attributed to the TiO_2 partial reduction by hydrogen spilt-over from the Pd. However, the permeation results were given at a lower operating temperature (500 °C), showing a H_2 permeance of $1.9 \cdot 10^{-3}$ mol s^{-1} $m^{-2} \cdot Pa^{-0.5}$ with H_2/N_2-selectivity around 800. The combined effect of time and temperature during permeation experiments were not addressed in that work.

To reveal the precise causes of this phenomenon, an exhaustive analysis of the membrane was carried out after the long-term permeation experiments. The cross-section of membranes containing based-TiO_2 intermediate layers (TiO_2/Pd and Pd–TiO_2/Pd) after the entire set of permeation experiments (particularly around one thousand hours of continuous operation for Pd–TiO_2/Pd) were analyzed by scanning electron microscopy combined with energy-dispersive X-ray spectroscopy.

A homogeneous and fully dense Pd top film can be observed on the external surface of both membranes, as previously explained in section Membrane morphology, although with a significant variation for its thickness. In fact, this top coating is noticeably lower for Pd–TiO_2/Pd if compared with TiO_2/Pd, although a greater penetration of palladium into some pores of the support close to the external side was also obtained. Analyzing in detail these values, a real Pd-thickness in the top film of around 10–14 μm and only 2.9 μm were reached for TiO_2/Pd and Pd–TiO_2/Pd, respectively. These real values are remarkably lower than that of the estimated ones by gravimetric analysis, 19.4 and 9.7 μm, respectively. It can be explained by the partial Pd infiltration inside the pores, especially in the case of analyzing the membrane Pd–TiO_2/Pd, where a thickness reduction of 69% in the top Pd-film was found but the metal was also incorporated into the pores up to around 50 μm in depth. This fact corroborates the preliminary hypothesis given while analyzing the permeation behavior of these membranes, based on a thicker effective distance in the bulk palladium that hydrogen needs to pass through during permeation that leads to an overall lower permeation capacity. On the other contrary, precisely this palladium infiltration into the pores improves the anchorage of the Pd-film to the porous substrate, thus enhancing the mechanical resistance of the composite structure.

Further analyses were carried out for Pd–TiO_2/Pd, which was tested around one thousand hours of continuous operation. A certain decrease of the permeation capacity was reached after operating at 450 °C, although excellent mechanical integrity was maintained during the entire set of

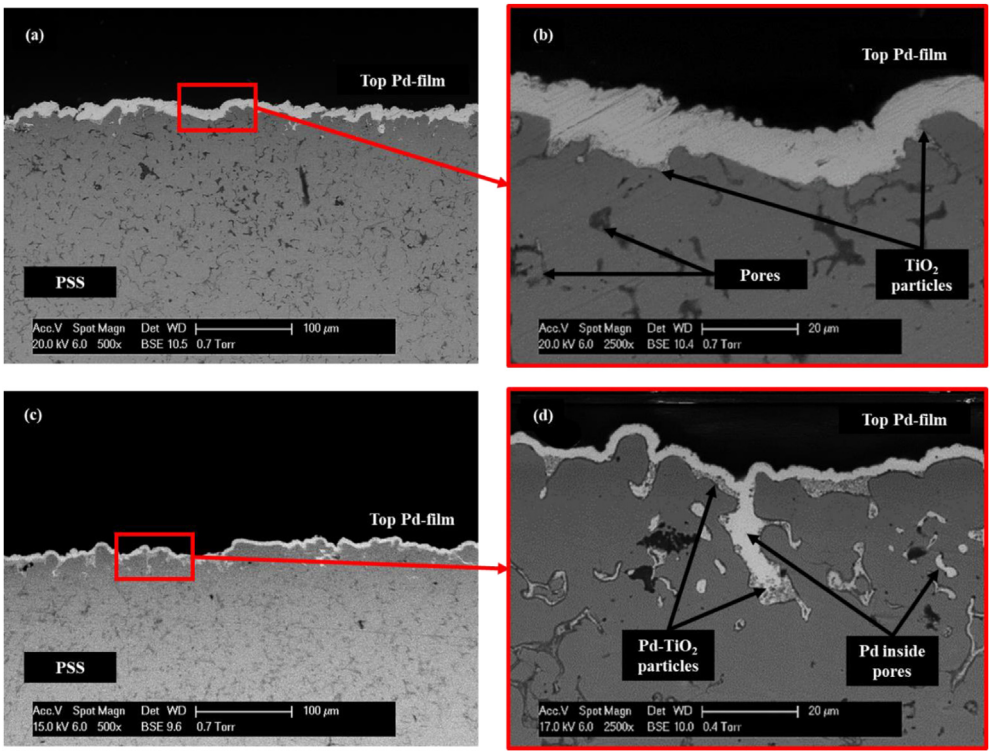

Fig. 10 – Cross-section micrographs of membranes after permeation experiments at different magnification: TiO_2/Pd (a, b) and Pd–TiO_2/Pd (c, d).

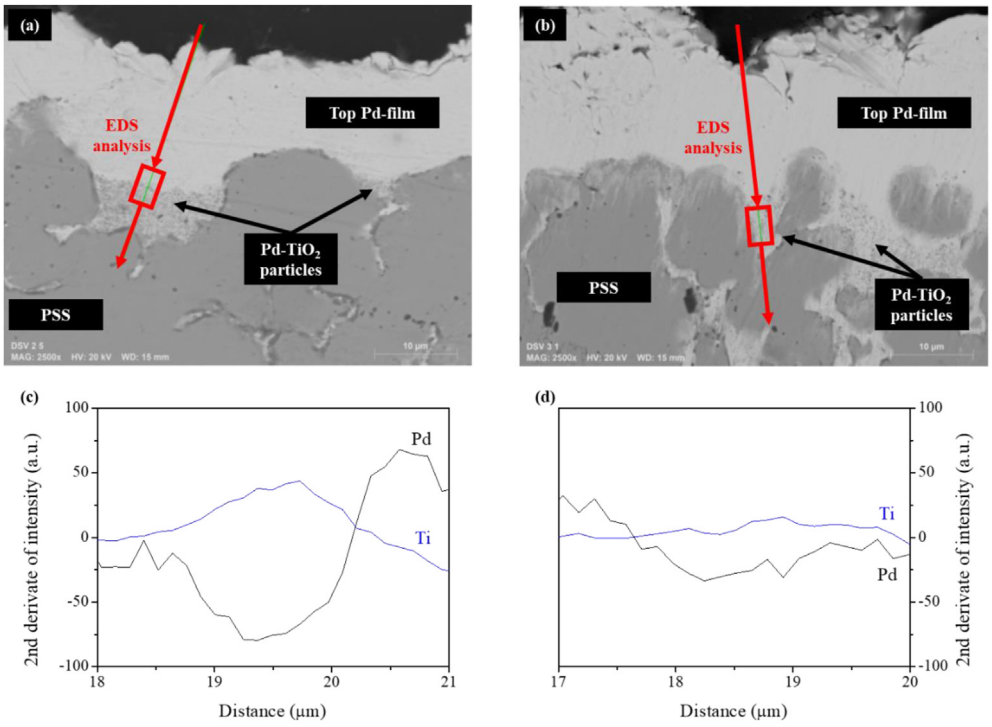

Fig. 11 – Composition analysis in the radial direction for Pd–TiO_2/Pd membrane before (a, c) and after (b, d) permeation tests.

experiments. The composition of the Pd-film in the radial direction of analogous membranes was determined by EDS analyses before and after permeation tests. Here, the most relevant results are shown in Fig. 11, where the composition data was processed to obtain the second derivate of signals for palladium and titanium. This calculation provides information about the maximum velocity of concentration variation of these elements in the radial direction. A total distance of 3 μm in the radial direction was selected for the analysis, just around the area between palladium and intermediate layer are intimately in contact. The original results obtained from EDS analysis without any data handling are collected as supplementary information in Figs. S2 and S3. Focusing on the results reached before permeation tests (Fig. 10a and c), a contrary behavior of signals assigned to each element, palladium and titanium, was found. In this manner, the intensity of the second derivate starts decreasing for palladium around 19 μm in depth and simultaneously increases for titanium. This trend switches after around 1 μm, increasing the palladium signal while decreasing the titanium signal. It indicates the transition between the fully dense palladium film and TiO_2 particles incorporated onto the PSS support as intermediate layer. The marked simultaneous variation in the intensity of composition second derivate suggests a minimal interaction between both elements, palladium and titanium. On the contrary, moving to the membrane analyzed after long-term permeation tests at high temperatures (Fig. 10b and d), certainly flat response was reached for the composition second derivate. It suggests a very slight variation in the composition around the area in which both palladium and TiO_2 particles are in intimate contact and, hence, a possible alloy between both metals. In this context, it should be noted that this possible alloy could not be detected clearly by DRX analysis due to the very low concentration of titanium into the alloy. However, this fact could explain the H_2-permeance decrease of these membranes when operating at temperatures of around 450 °C.

Besides, despite the above-mentioned possible interaction between palladium and titanium at temperatures above 450 °C, this work demonstrates the excellent mechanical and operating stability of Pd–TiO_2/Pd membranes prepared by ELP-PP for several hundred hours while maintaining temperatures slightly lower around 400 °C. It provides a good potential of these membranes for certain applications, such as independent separators or membrane reactors operating at moderate temperatures.

Conclusions

In this work, two different Pd-based membranes prepared by Electroless Pore-Plating onto PSS support modified with TiO_2 particles have been successfully fabricated. Both morphology and performance of these membranes have been compared when using raw TiO_2 or TiO_2 particles doped with Pd nuclei as intermediate layer. The previous activation of the ceramic particles before their incorporation onto the PSS support caused a reduction of the Pd amount required to reach a fully dense membrane. In this manner, Pd layer thicknesses of 9.7 and 19.4 μm were obtained for TiO_2/Pd and Pd–TiO_2/Pd, respectively, as estimated by gravimetric analysis. However, the real values were noticeably lower due to the partial infiltration of Pd inside the pores. It was especially marked for Pd–TiO_2/Pd, in which a top Pd-film below 3 μm was observed

with a certain penetration inside external pores of the support up to around 50 μm in depth in some points. However, this lower thickness did not cause an increase in the permeation capacity, precisely due to the infiltration mentioned above of palladium inside the pores. Thus, H_2-permeances of around $4.16 \cdot 10^{-4}$ and $2.97 \cdot 10^{-4}$ mol s^{-1} m^{-2} $Pa^{-0.5}$ at 400 °C were reached for TiO_2/Pd and Pd–TiO_2/Pd, respectively. Despite this fact, the better mechanical stability of the composite structure was found for the membrane prepared with previously doped Pd–TiO_2 particles, maintaining complete hydrogen selectivity at multiple operating conditions for almost 1000 h, even permeating from the inner to the outer surface of the membrane (in-out mode) and generating tensile stress on the composite structure.

The presence of nitrogen in the feed stream causes a certain decrease in the H_2-permeance due to concentration-polarization, especially in the case of operating accordingly to the in-out mode. However, this configuration exhibits a more effective solution in the case of using sweep gas to maximize the pressure driving force during experiments.

Finally, the long-term stability of Pd–TiO_2/Pd in terms of hydrogen permeation has been determined between 400 and 450 °C. In this manner, very stable permeate fluxes were found for temperatures of around 400 °C, always recovering the initial permeation behavior after eventual alternations generated by feeding binary mixtures or switching the permeate flux direction. However, an irreversible permeation decrease has been obtained when operating at 450 °C, which can be explained by a possible alloy between palladium and titanium. However, it should be emphasized that the complete H_2-selectivity was also maintained in this case. Thus, the present work demonstrates the potential of Pd–TiO_2/Pd membranes prepared by ELP-PP to be used in either independent separators or membrane reactors if moderate temperatures are maintained.

Declaration of competing interest

The authors declare that they have no known competing financial interests or personal relationships that could have appeared to influence the work reported in this paper.

Acknowledgements

The authors hugely thank the financial support provided by the Spanish government through the competitive project ENE2017-83696-R to complete the current research. Moreover, we would also like to express our gratitude to the Microscopy Unit from SIdI at Universidad Autónoma de Madrid for the SEM micrographs and EDS analyses.

Appendix A. Supplementary data

Supplementary data to this article can be found online at https://doi.org/10.1016/j.ijhydene.2021.12.005.

REFERENCES

[1] Abe JO, Popoola API, Ajenifuja E, Popoola OM. Hydrogen energy, economy and storage: review and recommendation. Int J Hydrogen Energy 2019;44:15072–86. https://doi.org/10.1016/j.ijhydene.2019.04.068.
[2] Sazali N. Emerging technologies by hydrogen: a review. Int J Hydrogen Energy 2020;45:18753–71. https://doi.org/10.1016/j.ijhydene.2020.05.021.
[3] da Silva Veras T, Mozer TS, da Costa Rubim Messeder dos Santos D, da Silva César A. Hydrogen: trends, production and characterization of the main process worldwide. Int J Hydrogen Energy 2017;42:2018–33. https://doi.org/10.1016/j.ijhydene.2016.08.219.
[4] Muradov NZ, Veziroğlu TN. "Green" path from fossil-based to hydrogen economy: an overview of carbon-neutral technologies. Int J Hydrogen Energy 2008;33:6804–39. https://doi.org/10.1016/j.ijhydene.2008.08.054.
[5] Anwar S, Khan F, Zhang Y, Djire A. Recent development in electrocatalysts for hydrogen production through water electrolysis. Int J Hydrogen Energy 2021;46:32284–317. https://doi.org/10.1016/j.ijhydene.2021.06.191.
[6] Orfila M, Sanz D, Linares M, Molina R, Sanz R, Marugán J, et al. H2 production by thermochemical water splitting with reticulated porous structures of ceria-based mixed oxide materials. Int J Hydrogen Energy 2020;6. https://doi.org/10.1016/j.ijhydene.2020.04.222.
[7] Sarangi PK, Nanda S. Biohydrogen production through dark fermentation. Chem Eng Technol 2020;43:601–12. https://doi.org/10.1002/ceat.201900452.
[8] Farzad S, Mandegari MA, Görgens JF. A critical review on biomass gasification, co-gasification, and their environmental assessments. Biofuel Res J 2016;3:483–95. https://doi.org/10.18331/BRJ2016.3.4.3.
[9] Megía PJ, Carrero A, Calles JA, Vizcaíno AJ. Hydrogen production from steam reforming of acetic acid as a model compound of the aqueous fraction of microalgae HTL using Co-M/SBA-15 (M: Cu, Ag, Ce, Cr) catalysts. Catalysts 2019;9. https://doi.org/10.3390/catal9121013.
[10] Calles JA, Carrero A, Vizcaíno AJ, García-Moreno L, Megía PJ. Steam reforming of model bio-oil aqueous fraction using Ni-(Cu, Co, Cr)/SBA-15 catalysts. Int J Mol Sci 2019;20. https://doi.org/10.3390/ijms20030512.
[11] Nazir H, Louis C, Jose S, Prakash J, Muthuswamy N, Buan MEM, et al. Is the H2 economy realizable in the foreseeable future? Part I: H2 production methods. Int J Hydrogen Energy 2020;45:13777–88. https://doi.org/10.1016/j.ijhydene.2020.03.092.
[12] Nikolaidis P, Poullikkas A. A comparative overview of hydrogen production processes. Renew Sustain Energy Rev 2017;67:597–611. https://doi.org/10.1016/j.rser.2016.09.044.
[13] Peighambardoust SJ, Rowshanzamir S, Amjadi M. Review of the proton exchange membranes for fuel cell applications, vol. 35. Elsevier Ltd; 2010. https://doi.org/10.1016/j.ijhydene.2010.05.017.
[14] Yáñez M, Relvas F, Ortiz A, Gorri D, Mendes A, Ortiz I. PSA purification of waste hydrogen from ammonia plants to fuel cell grade. Separ Purif Technol 2020;240:116334. https://doi.org/10.1016/j.seppur.2019.116334.
[15] Al-Mufachi NA, Rees Nv, Steinberger-Wilkens R. Hydrogen selective membranes: a review of palladium-based dense metal membranes. Renew Sustain Energy Rev 2015;47:540–51. https://doi.org/10.1016/j.rser.2015.03.026.
[16] Orakwe I, Shehu H, Gobina E. Preparation and characterization of palladium ceramic alumina membrane for hydrogen

permeation. Int J Hydrogen Energy 2019;44:9914–21. https://doi.org/10.1016/j.ijhydene.2019.01.033.
[17] Anzelmo B, Liguori S, Mardilovich I, Iulianelli A, Ma YH, Wilcox J, et al. Fabrication & performance study of a palladium on alumina supported membrane reactor: natural gas steam reforming, a case study. Int J Hydrogen Energy 2018;43:7713–21. https://doi.org/10.1016/j.ijhydene.2017.08.164.
[18] Lu GQ, Diniz da Costa JC, Duke M, Giessler S, Socolow R, Williams RH, et al. Inorganic membranes for hydrogen production and purification: a critical review and perspective. J Colloid Interface Sci 2007;314:589–603. https://doi.org/10.1016/j.jcis.2007.05.067.
[19] Mendes D, Chibante V, Zheng JM, Tosti S, Borgognoni F, Mendes A, et al. Enhancing the production of hydrogen via water-gas shift reaction using Pd-based membrane reactors. Int J Hydrogen Energy 2010;35:12596–608. https://doi.org/10.1016/j.ijhydene.2010.07.159.
[20] Gallucci F, Fernandez E, Corengia P, van Sint Annaland M. Recent advances on membranes and membrane reactors for hydrogen production. Chem Eng Sci 2013. https://doi.org/10.1016/j.ces.2013.01.008.
[21] Rahimpour MR, Samimi F, Babapoor A, Tohidian T, Mohebi S. Palladium membranes applications in reaction systems for hydrogen separation and purification: a review. Chem Eng Process: Process Intensification 2017;121:24–49. https://doi.org/10.1016/j.cep.2017.07.021.
[22] Peters T, Caravella A. Pd-based membranes: overview and perspectives. Membranes 2019;9:1–5. https://doi.org/10.3390/membranes9020025.
[23] Lytkina AA, Orekhova Nv, Yaroslavtsev AB. Methanol steam reforming in membrane reactors. Petrol Chem 2018;58:911–22. https://doi.org/10.1134/S096554411811004X.
[24] Anzelmo B, Wilcox J, Liguori S. Hydrogen production via natural gas steam reforming in a Pd-Au membrane reactor. Comparison between methane and natural gas steam reforming reactions. J Membr Sci 2018;568:113–20. https://doi.org/10.1016/j.memsci.2018.09.054.
[25] Caravella A, Barbieri G, Drioli E. Modelling and simulation of hydrogen permeation through supported Pd-alloy membranes with a multicomponent approach. Chem Eng Sci 2008;63:2149–60. https://doi.org/10.1016/j.ces.2008.01.009.
[26] Plazaola AA, Tanaka DAP, Annaland MVS, Gallucci F. Recent advances in pd-based membranes for membrane reactors. Molecules 2017;22:1–53. https://doi.org/10.3390/molecules22010051.
[27] Alique D, Martinez-Diaz D, Sanz R, Calles JA. Review of supported pd-based membranes preparation by electroless plating for ultra-pure hydrogen production. Membranes 2018;8:1–39. https://doi.org/10.3390/membranes8010005.
[28] Dittmeyer R, Höllein V, Daub K. Membrane reactors for hydrogenation and dehydrogenation processes based on supported palladium. J Mol Catal Chem 2001;173:135–84. https://doi.org/10.1016/S1381-1169(01)00149-2.
[29] Hu X, Chen W, Huang Y. Fabrication of Pd/ceramic membranes for hydrogen separation based on low-cost macroporous ceramics with pencil coating. Int J Hydrogen Energy 2010;35:7803–8. https://doi.org/10.1016/j.ijhydene.2010.05.102.
[30] Bottino A, Broglia M, Capannelli G, Comite A, Pinacci P, Scrignari M, et al. Sol-gel synthesis of thin alumina layers on porous stainless steel supports for high temperature palladium membranes. Int J Hydrogen Energy 2014;39:4717–24. https://doi.org/10.1016/j.ijhydene.2013.11.096.
[31] Sanz R, Calles JA, Alique D, Furones L, Ordóñez S, Marín P, et al. Preparation, testing and modelling of a hydrogen selective Pd/YSZ/SS composite membrane. Int J Hydrogen Energy 2011;36:15783–93. https://doi.org/10.1016/j.ijhydene.2011.08.102.
[32] Chi YH, Yen PS, Jeng MS, Ko ST, Lee TC. Preparation of thin Pd membrane on porous stainless steel tubes modified by a two-step method. Int J Hydrogen Energy 2010;35:6303–10. https://doi.org/10.1016/j.ijhydene.2010.03.066.
[33] Huang Y, Dittmeyer R. Preparation and characterization of composite palladium membranes on sinter-metal supports with a ceramic barrier against intermetallic diffusion. J Membr Sci 2006;282:296–310. https://doi.org/10.1016/j.memsci.2006.05.032.
[34] Calles JA, Sanz R, Alique D. Influence of the type of siliceous material used as intermediate layer in the preparation of hydrogen selective palladium composite membranes over a porous stainless steel support. Int J Hydrogen Energy 2012;37:6030–42. https://doi.org/10.1016/j.ijhydene.2011.12.164.
[35] Su C, Jin T, Kuraoka K, Matsumura Y, Yazawa T. Thin palladium film supported on SiO2-modified porous stainless steel for a high-hydrogen-flux membrane. Ind Eng Chem Res 2005;44:3053–8. https://doi.org/10.1021/ie049349b.
[36] Calles JA, Sanz R, Alique D, Furones L. Thermal stability and effect of typical water gas shift reactant composition on H2 permeability through a Pd-YSZ-PSS composite membrane. Int J Hydrogen Energy 2014;39:1398–409. https://doi.org/10.1016/j.ijhydene.2013.10.168.
[37] Kiadehi AD, Taghizadeh M. Fabrication, characterization, and application of palladium composite membrane on porous stainless steel substrate with NaY zeolite as an intermediate layer for hydrogen purification. Int J Hydrogen Energy 2019;44:2889–904. https://doi.org/10.1016/j.ijhydene.2018.12.058.
[38] Mobarake MD, Samiee L. Preparation of palladium/NaX/PSS membrane for hydrogen separation. Int J Hydrogen Energy 2016;41:79–86. https://doi.org/10.1016/j.ijhydene.2015.10.009.
[39] Qiao A, Zhang K, Tian Y, Xie L, Luo H, Lin YS, et al. Hydrogen separation through palladium-copper membranes on porous stainless steel with sol-gel derived ceria as diffusion barrier. Fuel 2010;89:1274–9. https://doi.org/10.1016/j.fuel.2009.12.006.
[40] Wei L, Yu J, Hu X, Huang Y. Facile surface modification of porous stainless steel substrate with TiO2intermediate layer for fabrication of H2-permeable composite palladium membranes. Separ Sci Technol 2016;51:998–1006. https://doi.org/10.1080/01496395.2015.1136330.
[41] Haider AJ, Jameel ZN, Al-Hussaini IHM. Review on: titanium dioxide applications. Energy Procedia 2019;157:17–29. https://doi.org/10.1016/j.egypro.2018.11.159.
[42] Mamaghani AH, Haghighat F, Lee CS. Role of titanium dioxide (TiO2) structural design/morphology in photocatalytic air purification. Appl Catal B Environ 2020;269. https://doi.org/10.1016/j.apcatb.2020.118735.
[43] Fernandez E, Helmi A, Coenen K, Melendez J, Viviente JL, Pacheco Tanaka DA, et al. Development of thin Pd-Ag supported membranes for fluidized bed membrane reactors including WGS related gases. Int J Hydrogen Energy 2015;40:3506–19. https://doi.org/10.1016/j.ijhydene.2014.08.074.
[44] Arratibel A, Pacheco Tanaka A, van Sint Annaland M, Gallucci F. On the use of double-skinned membranes to prevent chemical interaction between membranes and catalysts. Int J Hydrogen Energy 2021;46:20240–4. https://doi.org/10.1016/j.ijhydene.2019.10.203.
[45] Furones L, Alique D. Interlayer properties of in-situ oxidized porous stainless steel for preparation of composite Pd membranes. Chem Eng 2017;1:2. https://doi.org/10.3390/chemengineering2010001.
[46] Calles JA, Sanz R, Alique D, Furones L, Marín P, Ordoñez S. Influence of the selective layer morphology on the

permeation properties for Pd-PSS composite membranes prepared by electroless pore-plating: experimental and modeling study. Separ Purif Technol 2018;194:10–8. https://doi.org/10.1016/j.seppur.2017.11.014.

[47] Sanz R, Calles JA, Ordóñez S, Marín P, Alique D, Furones L. Modelling and simulation of permeation behaviour on Pd/PSS composite membranes prepared by "pore-plating" method. J Membr Sci 2013;446:410–21. https://doi.org/10.1016/j.memsci.2013.06.060.

[48] Sanz-Villanueva D, Alique D, Vizcaíno AJ, Sanz R, Calles JA. Pre-activation of SBA-15 intermediate barriers with Pd nuclei to increase thermal and mechanical resistances of pore-plated Pd-membranes. Int J Hydrogen Energy 2021;46:20198–212. https://doi.org/10.1016/j.ijhydene.2020.07.028.

[49] Maroño M, Alessandro G, Morales A, Martinez-Diaz D, Alique D, Sánchez JM. Influence of Si and Fe/Cr oxides as intermediate layers in the fabrication of supported Pd membranes. Separ Purif Technol 2020;234. https://doi.org/10.1016/j.seppur.2019.116091.

[50] Martinez-Diaz D, Sanz R, Calles JA, Alique D. H 2 permeation increase of electroless pore-plated Pd/PSS membranes with CeO 2 intermediate barriers. Separ Purif Technol 2019;216:16–24. https://doi.org/10.1016/j.seppur.2019.01.076.

[51] Sanz R, Calles JA, Alique D, Furones L. New synthesis method of Pd membranes over tubular PSS supports via "pore-plating" for hydrogen separation processes. Int J Hydrogen Energy 2012;37:18476–85. https://doi.org/10.1016/j.ijhydene.2012.09.084.

[52] Martinez-Diaz D, Alique D, Calles JA, Sanz R. Pd-thickness reduction in electroless pore-plated membranes by using doped-ceria as interlayer. Int J Hydrogen Energy 2020;45:7278–89. https://doi.org/10.1016/j.ijhydene.2019.10.140.

[53] Alique D, Sanz R, Calles JA. Pd membranes by electroless pore-plating. Elsevier Inc.; 2020. https://doi.org/10.1016/b978-0-12-818332-8.00002-8.

[54] Alique D, Imperatore M, Sanz R, Calles JA. Hydrogen permeation in composite Pd-membranes prepared by conventional electroless plating and electroless pore-plating alternatives over ceramic and metallic supports. Int J Hydrogen Energy 2016;41:19430–8. https://doi.org/10.1016/j.ijhydene.2016.06.128.

[55] Liguori S, Iulianelli A, Dalena F, Pinacci P, Drago F, Broglia M, et al. Performance and long-term stability of Pd/PSS and Pd/Al2O3 membranes for hydrogen separation. Membranes 2014;4:143–62. https://doi.org/10.3390/membranes4010143.

[56] Huang Y, Dittmeyer R. Preparation of thin palladium membranes on a porous support with rough surface. J Membr Sci 2007;302:160–70. https://doi.org/10.1016/j.memsci.2007.06.040.

[57] Bosko ML, Ojeda F, Lombardo EA, Cornaglia LM. NaA zeolite as an effective diffusion barrier in composite Pd/PSS membranes. J Membr Sci 2009;331:57–65. https://doi.org/10.1016/j.memsci.2009.01.005.

[58] Tong J, Matsumura Y, Suda H, Haraya K. Thin and dense Pd/CeO2/MPSS composite membrane for hydrogen separation and steam reforming of methane. Separ Purif Technol 2005;46:1–10. https://doi.org/10.1016/j.seppur.2005.03.011.

[59] Zhao C, Caravella A, Xu H, Brunetti A, Barbieri G, Goldbach A. Support mass transfer resistance of Pd/ceramic composite membranes in the presence of sweep gas. J Membr Sci 2018;550:365–76. https://doi.org/10.1016/j.memsci.2017.12.082.